Journal of Solid State Electrochemistry
https://doi.org/10.1007/s10008-023-05702-8

ORIGINAL PAPER

Cadmium sensing with bentonite-modified carbon paste electrode: electrochemical insights

Abdellah Mourak[1,2] · Mohamed Hajjaji[1] · Rachid Idoulhi[2] · Mohy-Eddine Khadiri[2] · Abdesselam Abouelfida[2]

Received: 23 June 2023 / Revised: 23 September 2023 / Accepted: 27 September 2023

Abstract

Electrochemical detection of cadmium cations in aqueous solutions using a bentonite-modified carbon paste as working electrode was investigated. For this purpose, cyclic voltammetry, square wave voltammetry, and electrochemical impedance spectroscopy techniques were used. The findings demonstrated that the electrode composed of 20 mass% bentonite manifested high detection sensitivity, and hydrochloric acid was the best suitable supporting electrolyte. Under these operating conditions, the electron transfer process was quasi-reversible. Also, it was found that the increase of pH resulted in the decrease of the anodic current density, likely because of partial immobilization of the cadmium-derivative species (Cd^{2+}, $Cd(OH)^{+}$) by negatively charged clay particles. Furthermore, a linear relationship was observed between the initial concentration of Cd^{2+} (up to 5×10^{-5} M) and the anodic current density. The latter signal markedly declined as the Cd^{2+} ion concentration approached the cation exchange capacity of the electrode (about 6×10^{-6} M). The use of high potential scan rate (> 50 mV/s) led to the cathodic peak vanishing presumably because of the decline in the electron transfer between Cd^{2+} ions and the electrode. The used electrode was regenerated by using salt solution and successfully reused. Moreover, the co-presence of cadmium and lead ions did not alter its electrochemical performance. The electrode-solution interface was equivalent to an electrical circuit comprising a constant phase element in parallel with a resistance and a Warburg diffusion regime.

Keywords Modified electrode · Bentonite · Carbon paste · Electrochemical detection · Cadmium · Cyclic voltammogram

Introduction

Cadmium ($_{48}Cd$) is a heavy metal found in different commercial items [1] as well as in soils [2–4]. It has a long biological half-life and is highly toxic for human and living organisms [5, 6]. Consequently, it is crucial to monitor the levels of Cd in aquatic environments, soils, and commercial products. Considering drinking water, the concentrations of Cd must remain below 3 µg L^{-1} [7]. In aqueous solutions, Cd^{2+} ions are the unique stable species at pH < 8. At pH > 8, the amount of Cd^{2+} drastically decreases, and $Cd(OH)^{+}$ ions together with $Cd(OH)_2$ species occur. In highly alkaline solutions (pH > 12), the amount of $Cd(OH)^{+}$ ions is negligible, and hydroxyl species ($Cd(OH)_3^{-}$, $Cd(OH)_4^{2-}$) becomes abundant [8]. Cd ions as well as heavy metal cations can be successfully monitored by spectrometric techniques [9, 10]. However, despite their high sensitivity, these techniques are costly and not easily deployable outside the laboratory setting [11]. Thereby, special attention has been devoted to the use of electrochemical sensors because of their advantages: on-site detection, less bulky, rapid response, high sensitivity, and low cost [9, 12]. The electrode is one of the main components of these sensing systems as the electronic signal from such a sensor is sensitive to the nature and the quantity of the target analyte. Electrochemical devices with ion-selective electrodes have been proven efficient for monitoring pH, among others [13]. Carbon paste-paraffin oil electrodes have been successfully used for heavy metal detection [14]. But, despite their good electrical conductivity and electrochemical properties, these electrodes are less selective and have limited sensitivity. In order to surmount these limitations, the carbon paste was mixed

✉ Abdellah Mourak
abdellah.mourak@edu.uca.ac.ma

1 Materials Science and Process Optimization Laboratory, Marrakech, Morocco

2 Laboratory of Applied Chemistry and Biomass, Department of Chemistry, Faculty of Science Semlalia, University of Cadi Ayyad, BP 2390, Marrakech, Morocco

Published online: 05 October 2023

with materials characterized by good electrical, chemical, and mechanical properties [15–17]. Recently, it has been shown that nanomaterial-modified sensors are convenient for monitoring different chemical hazardous species, including heavy metals [18, 19]. The suitability of the nanomaterials, such as metal/metal oxide, synthesized polymers, carbon, and nanocomposites, is attributed in large part to their large surface/volume ratio and high surface reactivity. Because of their nanosized layers, chemical stability, lamellar structure, large specific surface area, and ability to exchange cations [20], smectite clay minerals are convenient materials for electrochemical sensor construction [21, 22]. As against to conventional electrodes, smectite-containing electrodes have been considered to be more efficient in electrocatalysis, electroanalysis, and preconcentration [23, 24]. Referring to the studies dealing with clay-based electrodes as sensing elements for heavy metal detection [25–27], the interaction between the studied metal species and these kinds of electrodes occurred by adsorption, intercalation, and/or cation exchange. Considering the published studies, which addressed the Cd cation detection by clay-modified electrode [28, 29], we noted that much less attention has been paid to the study of the operating factors such as solution pH, bentonite content, analyte concentration, electrolytes, and sweep rate on the electrochemical behavior of bentonite-containing sensors. In addition to its fundamental aspect, such a study could allow to maximize the sensor performances. On the other hand, there is a lack of studies which explained the electrochemical process in relation with the clay physico-chemical properties, i.e., cation exchange capacity (CEC). In addition, studies dealing with the regeneration and reuse of clay-modified electrodes have been ignored. Overall, no comprehensive electrochemical study involving Cd^{2+} ions and bentonite-carbon paste electrodes has been reported.

In light of the limitations of existing analytical techniques and the above-mentioned dearth of research on electrochemical methods for detecting cadmium (Cd), this study aimed to investigate the application of bentonite-modified carbon paste electrodes. For this purpose, the effects of the experiment operating factors, the regeneration and potential reuse of the electrodes, and their selectivity were investigated using cyclic voltammetry, square wave voltammetry, and electrochemical impedance spectroscopy.

Materials and methods

Identification and physical characteristics of the used clay

The clay material used was from the bentonite-rich area in the vicinity of the city of Nador (Morocco). It was ground and sieved (< 100 µm). Then, it was washed with a buffer solution (pH = 4.5) and sodium-saturated. The X-ray diffraction and the Fourier-transform infrared analyses of the raw and the Na-saturated clay (Fig. 1) showed that the clay was composed of smectite di-octahedral clay minerals (montmorillonite/beidellite), plagioclase, and quartz. The clay mineral amount exceeded 80 mass%. The chemical composition, the CEC, and the external surface area (SA) are given in Table 1. The chemical composition was determined by X-ray fluorescence spectrometry using an Axios-type spectrometer. The CEC value was measured by using cobaltihexamine cation

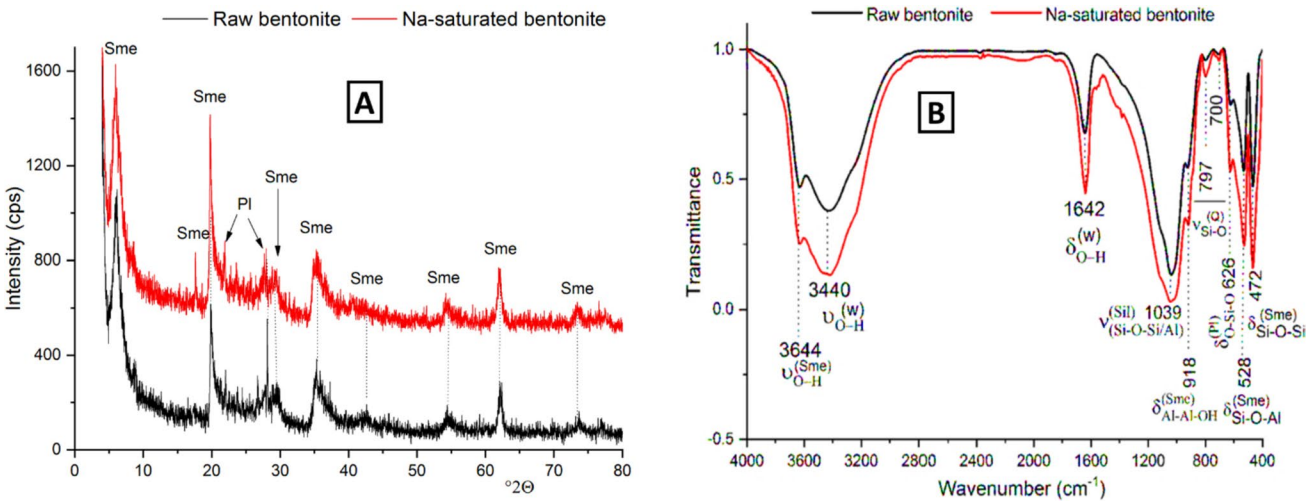

Fig. 1 X-ray diffraction patterns (**A**) and FT-IR spectra (**B**) of the raw and Na-saturated bentonite. Sme smectite, Pl plagioclase, Sil silicate, W water, Q quartz

Table 1 Chemical composition (mass%), cation exchange capacity (CEC), and external specific surface area (SA) of the studied bentonite

Chemical composition							CEC (meq/100 g)	SA (m^2/g)
SiO_2	Al_2O_3	Fe_2O_3	CaO	Na_2O	MgO	K_2O	60	54
62.89	26.85	3.31	2.62	1.63	1.51	0.67		

($[Co(NH_3)_6]^{3+}$) and following the procedure adopted by Aran et al. [29]. The external surface area was estimated by the BET (Brunauer-Emmett-Teller) method [30]. The somewhat high values of CEC and SA supported the abundance of the smectite clay minerals [31]. The iron and magnesium presence was taken as an indication of a partial substitution of the octahedral Al cations. The clay mineral charge compensation was achieved by sodium cations, among others.

Electrode construction procedure

The main steps followed for the bentonite-modified carbon paste electrode construction are indicated in Fig. 2. In relation with the bentonite addition, it should be noted the use of high amounts (> 20 mass% bentonite) led to the electrode peeling off. For the free-bentonite electrode construction, dried graphite powder (purity, 99%) and paraffin oil (85:15 mass/mass) were mixed and introduced in a PTFE carbon tube together with a wire conductor, as shown in Fig. 2. To determine the bentonite optimal amount, preliminary cyclic voltammetry tests were performed on the electrodes containing up to 20% bentonite. As can be deduced from Fig. 3, the detection sensitivity for Cd ions was better with the electrode composed of 20 mass% bentonite.

Supporting electrolytes and experimental conditions

The electrochemical behavior of the constructed electrodes regarding cadmium cation detection was investigated in acid (HCl, H_2SO_4) media and salt (NaCl, KCl)-containing aqueous solutions. The concentration of the supporting electrolytes was kept constant (0.1 M), and the initial concentration of Cd^{2+} ions was 10^{-3} M. Cadmium sulfate (purity, 99%) was used as Cd^{2+}-bearing compound.

The influence of the change of the analyte concentration (dynamic range, 5.10^{-6}–10^{-3} M) on the electrochemical behavior of the electrodes was investigated in the following conditions: pH = 2, electrolyte: HCl. The effect of pH was investigated in the range of 2 to 9. In this respect, it could be recalled that Cd^{2+} ions are the unique stable species in aqueous solutions with pH < 8, and both Cd^{2+} and $Cd(OH)^+$ are found at 8 < pH < 9 [32].

The effect of the sweep rate in cyclic voltammetry experiments was investigated in the 10–400 mV/s range.

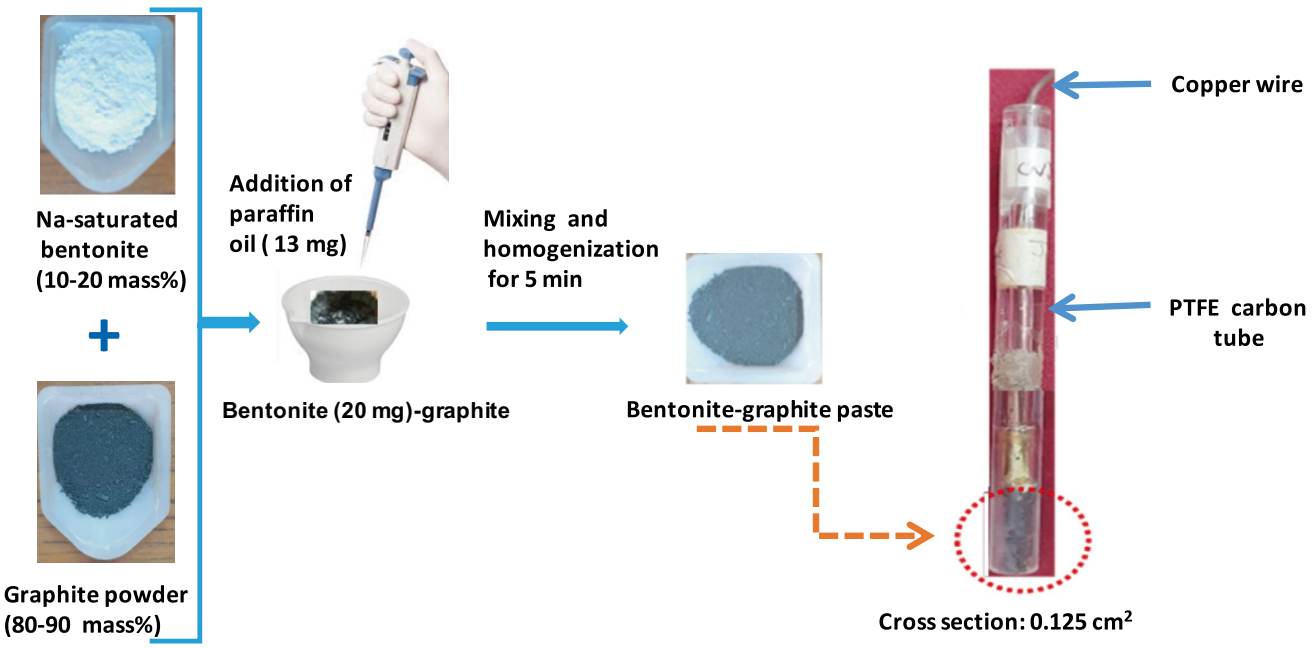

Fig. 2 Main steps followed for the electrode construction

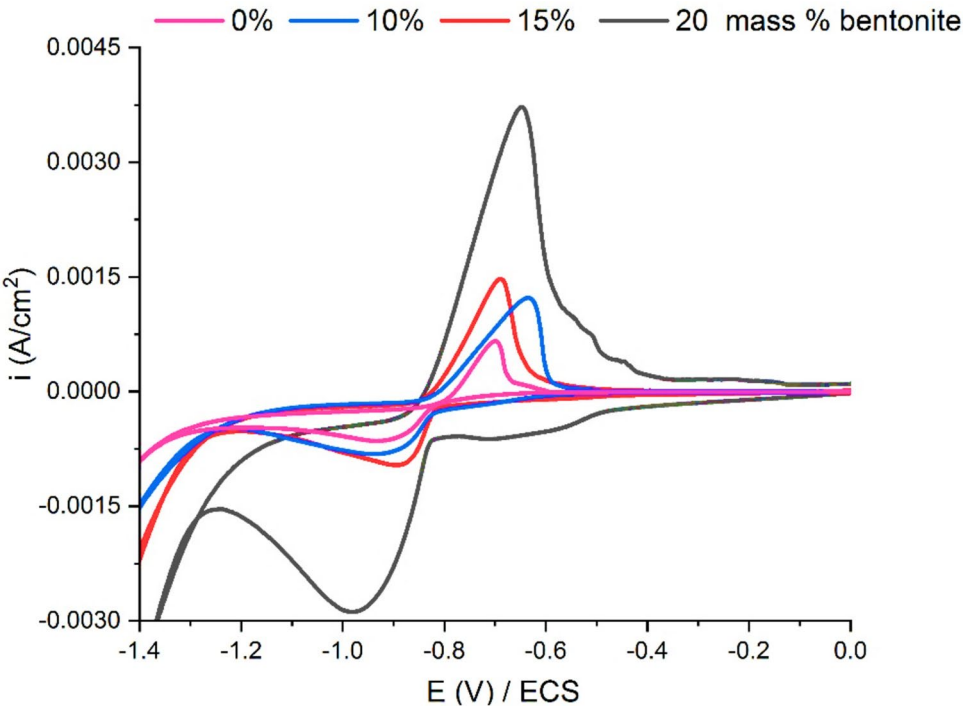

Fig. 3 Cyclic voltammograms obtained with bentonite-carbon paste electrodes composed of different amounts of bentonite. Cd^{2+} ion concentration, 10^{-3} M; electrolyte: HCl; pH = 2; sweep rate, 10 mV/s

HCl (0.1 M) was used as a supporting electrolyte. The Cd^{2+} ion concentration was of 10^{-3} M.

The limit of detection (LOD) and the limit of quantification (LOQ) of the studied electrode were determined according to the following relations [33]:

$$\mathrm{LOD} = 3S_B/S \quad (1)$$

$$\mathrm{LOQ} = 10S_B/S \quad (2)$$

where S_B is the standard deviation of 10 measurements taken from the signal obtained from the blank, and S is the slope of the calibration curve.

Electrochemical and characterization techniques

The electrochemical study was conducted using a potentiostat (CorrTest Electrochemical Workstation) connected to both a computer with CS Studio 5 software (for data processing) and an electrochemical cell. The cell was composed of the reference electrode (saturated calomel electrode—ECS), the working electrode (described in the "Electrode construction procedure" section) and a counter platinum electrode. The pH of the solution was monitored with a HI-2210 pH meter.

X-ray diffraction (XRD) analysis was performed on powder samples with a Rigaku SmartLab diffractometer operating with a copper anode ($\lambda_{K\alpha} = 1.5418$ Å). Fourier-transform infrared (FT-IR) analysis was conducted on thin discs (1 mg of sample and 99 mg of KBr) in the range of 4000–400 cm^{-1} using a Perkin-Elmer Fourier-Transform 1720-x-spectrophotometer. The microscopic examinations were carried out with a VEGA3 LM TESCAN scanning electron microscope coupled with EDS system. The samples were coated with a thin layer of carbon.

Results and discussion

Effect of supporting electrolytes

Values of relevant electrochemical parameters, determined from the cyclic voltammograms shown in Fig. 4, are given in Table 2. The anodic and cathodic current data showed that the peak ratio i_{pa}/i_{pc} deviated from unity (> 1) (Table 2) and the potential differences ΔE_p (mV) were > 59.2/n (n is the number of electrons transferred). These results together with the shape of the cyclic voltammograms allowed the deduction that the charge transfer process was quasi-reversible and no diffusion barrier could be conceivable [34–36].

The values of the ratio of the diffusion coefficients of the reduced (D_r), and the oxidized (D_o) forms, which were calculated from Eq. 3 [37], were insignificant ($D_r/D_o < 10^{-9}$) whatever the electrolyte used.

$$E_{1/2} = E^\circ + (RT/\mathrm{nF})\mathrm{Ln}(D_r/D_o)^{1/2} \quad (3)$$

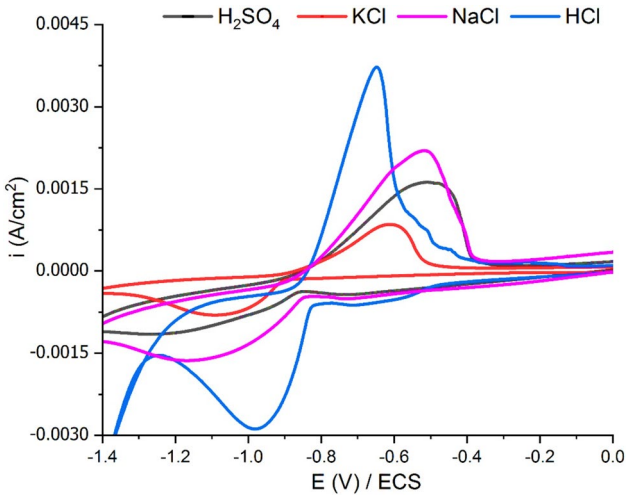

Fig. 4 Cyclic voltammograms related to the detection of Cd^{2+} ions with the studied electrode immersed in different electrolytes. Cd^{2+} ion concentration, 10^{-3} M; scan rate, 10 mV/s

where $E_{1/2}=(E_{pa}+E_{pc})/2$, $E°$ is the standard potential of Cd^{2+}/Cd at 25 °C (−0.646 V/ECS), R is the ideal gas constant ($R=8.31$ $JK^{-1}mol^{-1}$), F is the Faraday (96485.33 C/mol), and finally, n number of exchanged electrons ($n=2$).

Therefore, the diffusion coefficient of the reduced form was largely negligible. It was thought that the effect of the supporting electrolytes on the electrochemical behavior of the electrode did not have a relation with the interaction between cadmium species and electrolyte ions. It was rather tied to the extent of the clay mineral protonation and the cation exchange process. In this connection, it is worthy to note that SEM examination of the electrode tested in HCl solution revealed the presence of Cl, Na, and Cd (Fig. 5). The unexpected presence of Cl could be taken as an indication of the electrical balance of the protonated clay minerals. The detection of Cd associated with a drastic decrease of Na (about 70%) allowed us to suppose the substitution of Na^+ ions by Cd cations in all its forms [8, 38].

Effect of electrolyte solution pH

As can be drawn from the cyclic voltammograms shown in Fig. 6, the anodic and the cathodic current densities decreased with the increase of pH, and the ratio i_{pa}/i_{pc} fell within the interval 1–1.3. Moreover, the charge transfer was quasi-reversible in acidic solutions, but it was almost reversible in the basic medium. In acid solutions, Cd^{2+} ions are the unique stable species and the clay minerals are seemingly protonated as follows:

$$\equiv Al-OH + H^+ \rightarrow \equiv Al-OH_2^+ \rightarrow \equiv Al^+ + H_2O$$

Cd^{2+} ions could not be adsorbed on positively charged clay particles. Therefore, the main portion of the cations in solution should get involved in the electron transfer process. In such a condition, the current density increased. The change of the anodic current density against pH (≥ 4) followed the relation $i_{pa}=-0.23pH+3.10$ with a good correlation ($R^2_{Adj}=0.999$).

In alkaline solution, especially at pH = 9, both Cd^{2+} and $Cd(OH)^+$species should be present and the clay minerals were presumably deprotonated according to the following mechanism:

$$\equiv Al-OH + OH^- \rightarrow \equiv Al-(OH)_2^- \rightarrow \equiv Al-O^- + H_2O$$

Therefore, Cd^{2+} and $Cd(OH)^+$ ions were immobilized by the clay particles and could not be engaged in the electrochemical process. So, the current density decreased [39, 40].

Effect of the analyte concentration

The shape of the cyclic voltammograms obtained by operating with different Cd^{2+}-containing solutions was markedly influenced by changes in the Cd^{2+}ion concentration (Fig. 6). Moreover, the current signal intensity increased with the increase of Cd^{2+} ion concentration (Fig. 7). The broad range of the ratio i_{pa}/i_{pc}, 0.01–1.60, and the unsignificant

Table 2 Values of some relevant experimental and calculated electrochemical parameters. The experimental values were drawn from the cyclic voltammograms shown in Fig. 4

Electrolyte	Experimental parameters			Calculated parameters			
	[a]i_{pc} (mA/cm^2)	[b]i_{pa} (mA/cm^2)	[c]E_{pa} (V)	[d]E_{pc} (V)	i_{pa}/i_{pc}	[e]E_p (V)	[f]$E_{1/2}$ (V)
HCl	2.911 ± 0.019	3.778 ± 0.020	−0.648 ± 0.012	−0.983	1.297	−0.335	−0.815
NaCl	1.390 ± 0.013	2.200 ± 0.017	−0.519 ± 0.013	−1.021	1.582	−0.502	−0.770
H_2SO_4	0.964 ± 0.015	1.600 ± 0.019	−0.510 ± 0.018	−1.082	1.659	−0.572	−0.796
KCl	0.710 ± 0.021	0.860 ± 0.0022	−0.613 ± 0.012	−1.051	1.211	−0.438	−0.832

[a]Cathodic current density

[b]anodic current density

[c]anodic potential

[d]cathodic potential

[e]E_{pc}-E_{pa}

[f]half wave potential

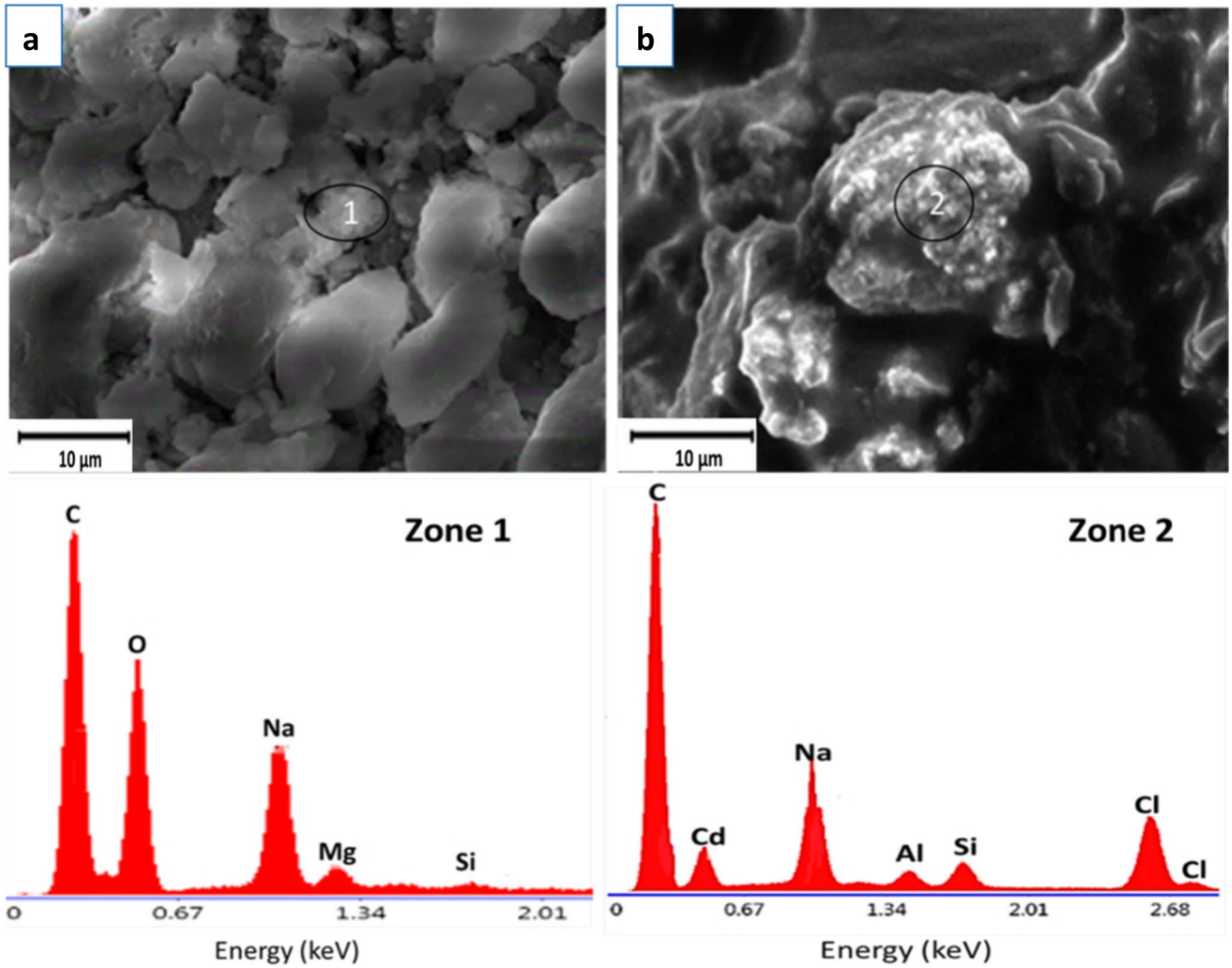

Fig. 5 SEM micrographs and EDX spectra of the studied electrode taken before (**a**, zone 1) and after (**b**, zone 2) use

D_t/D_o ratios ($5\times10^{-12} < D_t/D_o < 10^{-9}$), determined from the data retrieved from Fig. 7, showed how the electron and the mass transfers were affected by the change of Cd^{2+}ion concentration.

The curve representing the variation of the anodic current density (i_{pa}) against Ln(C_o) (C_o is the Cd^{2+} ion initial concentration) could be well decomposed into three branches (Fig. 8). In the Cd^{2+}concentration range of 5×10^{-4}–10^{-3} M, the current density variation followed the equation

$$i_{pa} = 3.98\mathrm{Ln}(C_o) + 31.08 \ (R^2{}_{\mathrm{Adj}} = 0.88) \quad (4)$$

In the interval 5×10^{-5}–5×10^{-4} M, it changed according to the relation

$$i_{pa} = 0.29\mathrm{Ln}(C_o) + 3.29 \ (R^2{}_{\mathrm{Adj}} = 0.99) \quad (5)$$

For low Cd^{2+} concentrations ($<5\times10^{-5}$ M), the i_{pa} variation was almost insignificant. In view of this result, the limit of detection should be slightly smaller than 5×10^{-5} M.

It was believed that the limit of detection was mainly limited by the bentonite cation exchange capacity (CEC). Indeed, taking into consideration the CEC value given in Table 1 and the bentonite mass used (20 mg), the Cd^{2+} amount, which could be involved in the CEC of the electrode, was estimated to be 6×10^{-6} mol. Thus, the amount of the Cd^{2+} ions in solutions with $C_o < 6\times10^{-6}$ M should be entirely immobilized by the electrode. In such a condition, the electron transfer is annihilated, and consequently, the anodic/cathodic peak current vanished.

The values of LOD and LOQ, which were determined by using Eqs. (1) and (2), were found to be 4.23×10^{-7} M and 1.41×10^{-6} M, respectively. It is noteworthy to note that

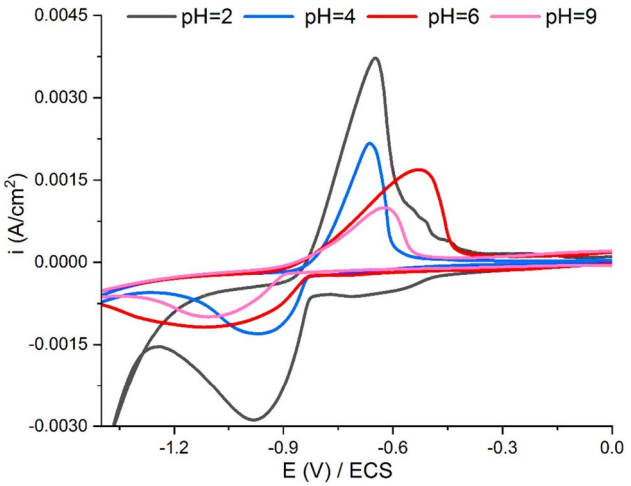

Fig. 6 Effect of the solution pH change on the shape of the cyclic voltammograms associated with Cd^{2+} ion detection with the studied electrode. Cd^{2+} ion concentration, 10^{-3} M; electrolyte: HCl; scan rate, 10 mV/s

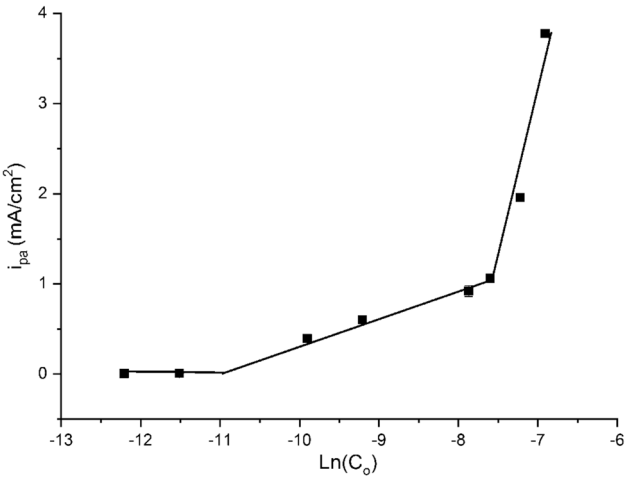

Fig. 8 Variation of the anodic current density against Ln(Co). Co: Cd^{2+} ion initial concentration

LOQ was close to the expected limit of detection (6×10^{-6} M) deduced on the basis of the CEC data.

Effect of potential sweep rate

The increase of the sweep rate led to the intensification of the anodic peak current together with a drastic drop of the cathodic current density (Fig. 9). So, the change of the sweep rate resulted in the electron transfer alteration. The current, which was presumably controlled by both the mass transport and the charge transfer at low scan rate, became determined by the electron transfer at high sweep rate. Otherwise, the electrochemical process, which was quasi-reversible at low-to-moderate sweep rates, became irreversible at $\nu > 50$ mV/s. The change in the electrochemical reversibility was supported by the parabolic trend of the curve: i_{pa} vs $\nu^{1/2}$ (Fig. 10). The disappearance of the cathodic peak current at $\nu > 50$ mV/s was believed to be due to the immobilization of the Cd^{2+} ions by the clay minerals principally by complexation (outer-sphere complexation). It was thought that at high sweep rates, the electron transfer between Cd^{2+} ions and the electrode was very slow as compared to the Cd^{2+} ion immobilization rate, and consequently, the cathodic reaction could not take place.

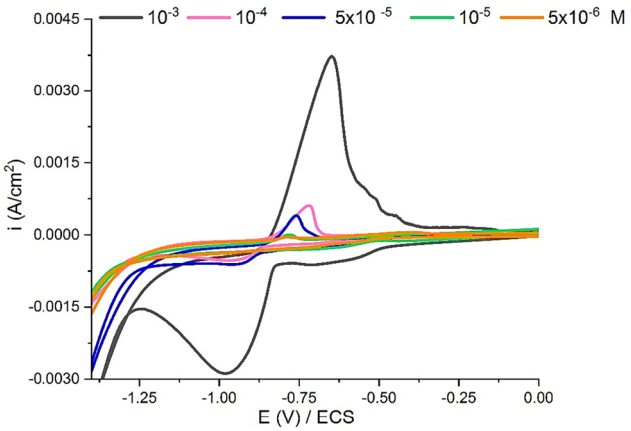

Fig. 7 Effect of the Cd^{2+} ion concentration change on the shape of the anodic and cathodic peaks. Electrode, 20 mass% bentonite-carbon paste; electrolyte: HCl; pH = 2; sweep rate, 10 mV/s

Equivalent circuit model of the electrode-solution interface

The Nyquist plots obtained for the bentonite-modified electrode and the carbon paste electrode in the presence of Cd^{2+} ions are given in Fig. 11. Considering these results, the electrochemical behavior of the electrodes/solution interfaces was equivalent to the electrical circuit shown in the inset of Fig. 11. Otherwise, the electrodes/electrolyte interfaces could be represented by the ratio $R_1+(Q_2/(R_2+W))$ (R_1 is the solution resistance, R_2 is the charge transfer resistance, Q_2 is the constant phase element, and W is the Warburg diffusion resistance [41]. The R_2 values for the bentonite-modified and the carbon paste electrodes were determined to be 14,254 and 52,756 Ω, respectively. The low R_2 value obtained for the bentonite-modified electrode was taken as an indication of high electron transfer between the solution and the studied electrode [42]. The Q_2 values determined for the carbon paste and the bentonite-modified electrodes were $0.141\times10^{-3}\ \mathrm{F\cdot s^{(a-1)}}$ and $52.76\times10^{-6}\ \mathrm{F\cdot s^{(a-1)}}$, respectively. The low Q_2 value was taken as an evidence for the accumulation of Cd cations on the surface of the

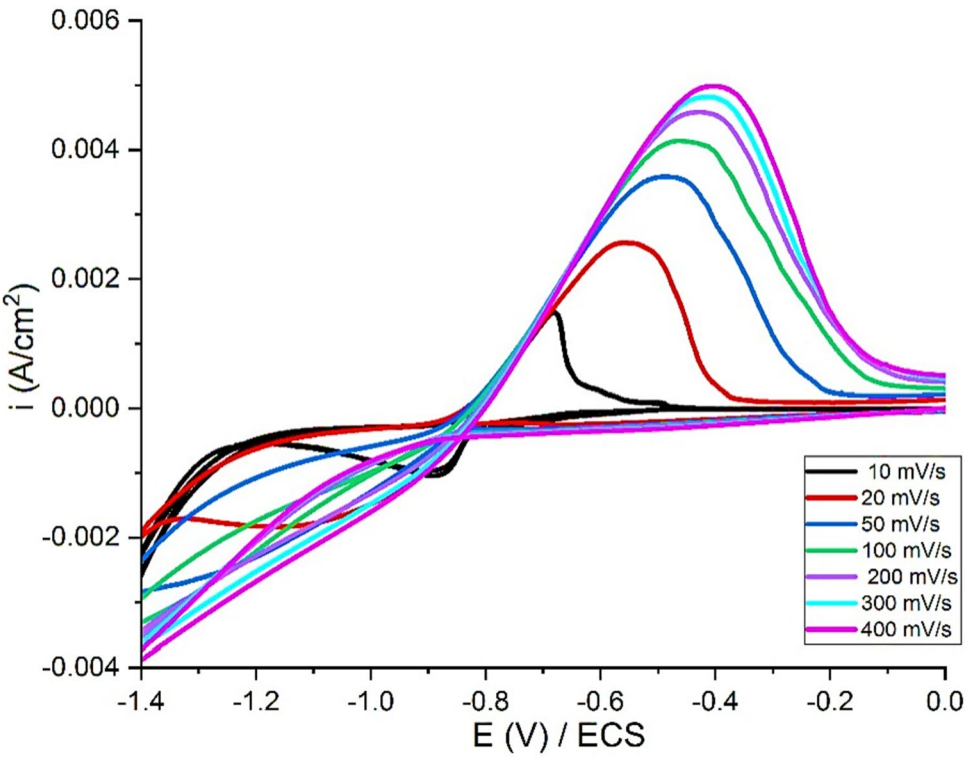

Fig. 9 Effect of the change of the potential scan rate on the shape of the cyclic voltammograms plotted by using the studied electrode. Cd^{2+} ion initial concentration, 10^{-3} M; electrolyte: HCl; pH = 2

bentonite-modified electrode [43, 44]. The *W* values for the carbon paste and the bentonite-modified electrodes were found to be 123.4 and 30.03 $\Omega/s^{-1/2}$, respectively. The higher *W* value for the carbon paste electrode suggested that the ions experienced some barrier to diffuse towards the electrode. In contrast, easier transfer of the ions occurred across the bentonite-modified electrode–electrolyte interface. In this respect, it is worth noting that the diffusion resistance Warburg feature manifested in the low-frequency region (< 35 Hz) of Nyquist diagrams (inset of Fig. 11).

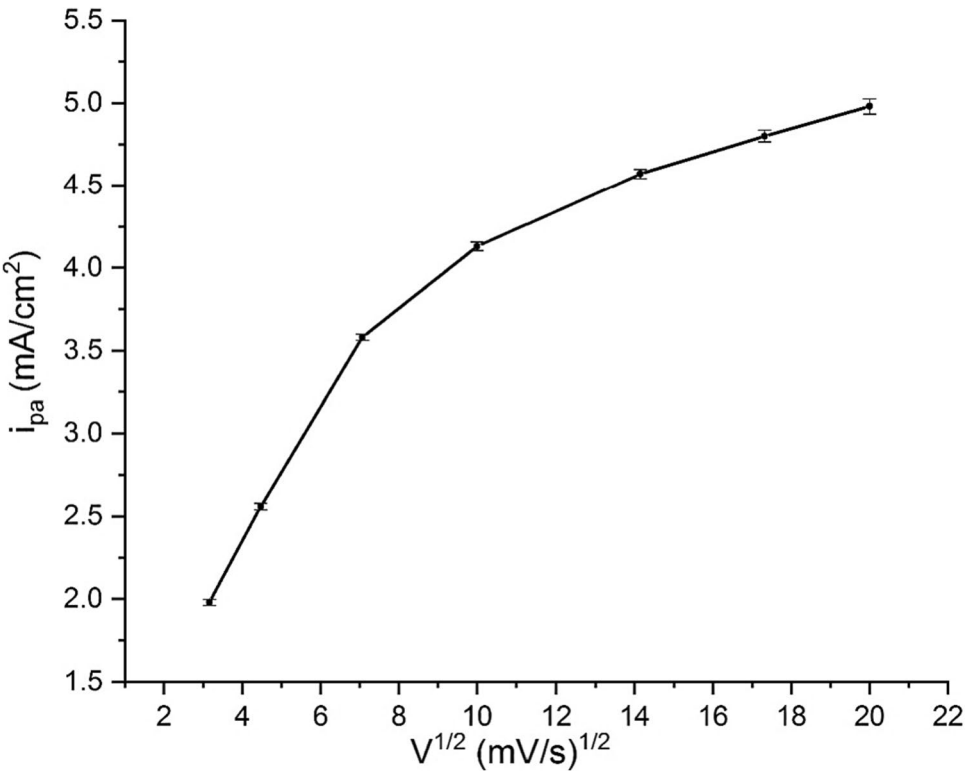

Fig. 10 Variation of the anodic current density versus the square root of the sweep rate

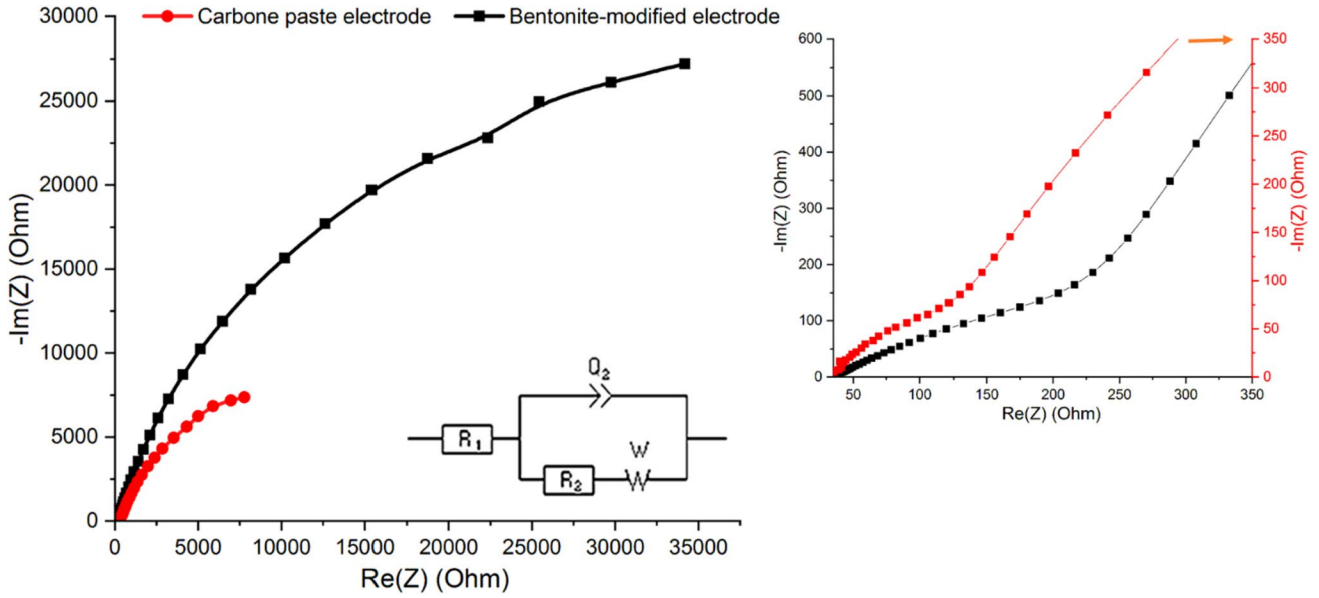

Fig. 11 Nyquist diagrams obtained by operating in the following conditions: electrodes: carbon paste and 20 mass% bentonite-carbon paste; electrolyte: HCl; pH = 2; Cd^{2+} ion concentration, 10^{-3} M

Regeneration and reuse of the electrode

The cyclic voltammogram plotted by operating with Cd^{2+}-free solution and using the bentonite-modified electrode, which has been already used for Cd^{2+} ion detection and immersed in NaCl solution (0.1 M) for 48 h, did not display any current signal associated with this metal (Fig. 12a). Conversely, the cyclic voltammogram obtained by using the Cd^{2+}-loaded bentonite-modified electrode closely resembled that obtained under normal experimental conditions (Cd^{2+}-containing solution, pristine bentonite-modified electrode) (Fig. 12b). These findings indicated that

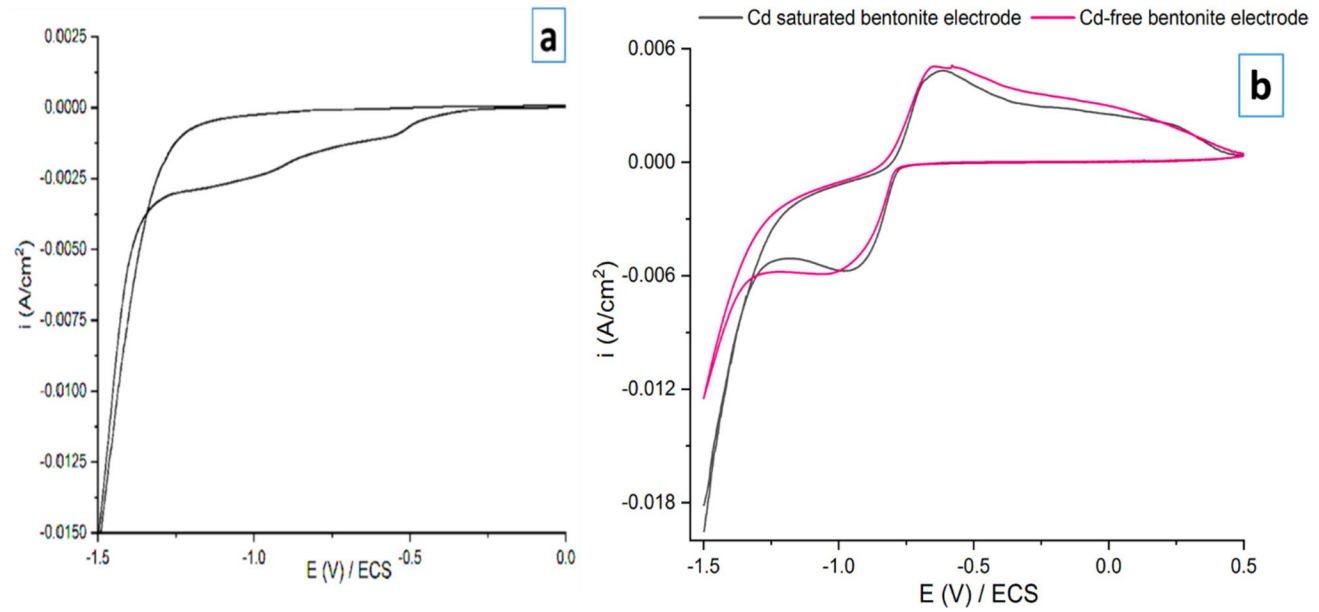

Fig. 12 Cyclic voltammograms obtained with different electrodes and by operating in Cd^{2+}-free and Cd^{2+}-containing solutions. **a** Regenerated and reused bentonite-modified electrode (Cd^{2+}-free aqueous solution). **b** Cd^{2+}-saturated bentonite-carbon paste electrode immersed in Cd^{2+}-free solution, and pristine bentonite-modified electrode submerged in Cd^{2+}-containing solution. pH = 2; electrolyte: HCl; sweep rate, 10 mV/s

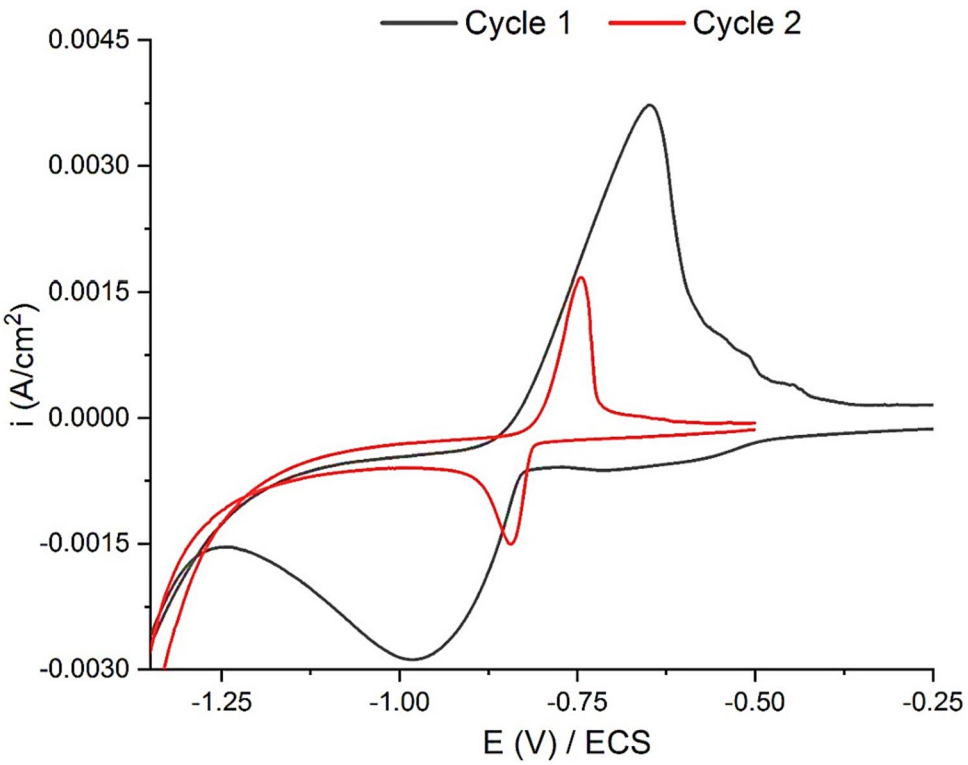

Fig. 13 Cyclic voltammograms plotted by using pristine (cycle 1) and reused (cycle 2) bentonite-modified electrode. Cd^{2+} ion initial concentration, 10^{-3} M; sweep rate, 10 mV/s; electrolyte: HCl; pH = 2

Cd cations were loosely tied to the electrode and they could be released by using NaCl solution.

The cyclic voltammetry experiments conducted on the regenerated electrode displayed anodic and cathodic current peaks related to the studied metal (Fig. 13). As compared with the pristine electrode signals, the peak intensities were substantially lessened and the potential positions were partially shifted. Considering, for instance, the cyclic voltammogram related to the second cycle, the variations of the currents intensities and the potentials were

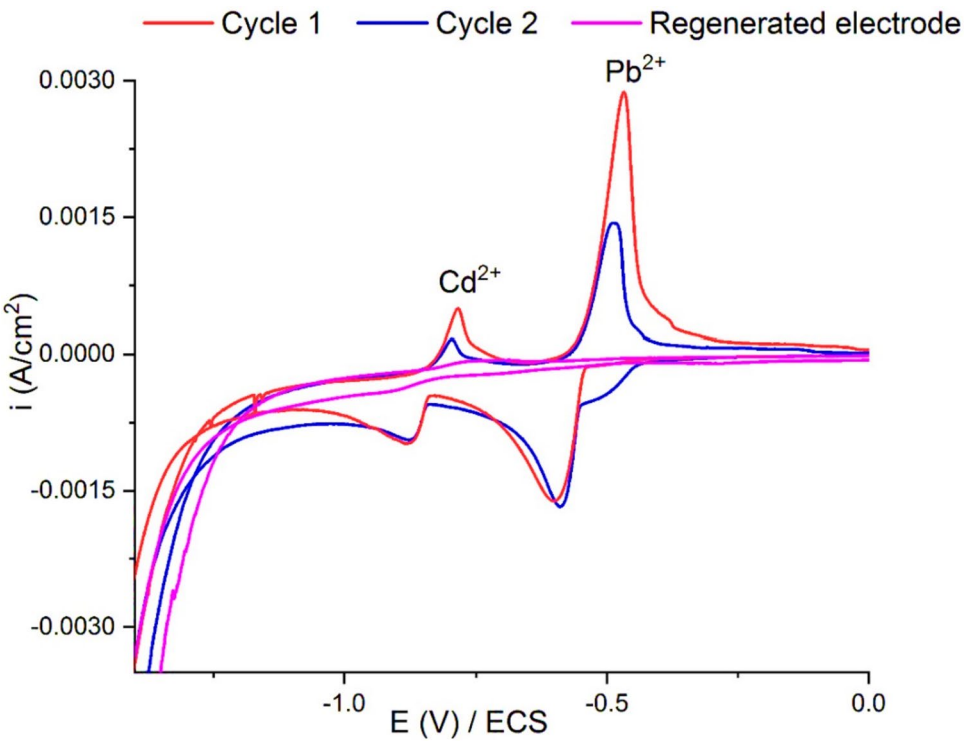

Fig. 14 Cyclic voltammograms related to the Cd^{2+} and Pb^{2+} ion detection by using the reused bentonite-modified electrode (cycles 1 and 2). The cyclic voltammogram corresponding to the regenerated electrode immersed in cation-free solution is introduced for comparison. Ion initial concentration, 10^{-3} M; sweep rate, 10 mV/s; electrolyte: HCl; pH = 2

$\Delta i_{pc} = 41\%, \Delta i_{pa} = 52\%, \Delta E_{pc} = 17\%, \Delta E_{pa} = 15\%$. The ratio i_{pa}/i_{pc}, which was obtained by using the data associated with the reused electrode, approached 1. Therefore, it was believed that the charge transfer changed from a quasi-reversible state to a reversible one, and it became relatively fast.

The bentonite-modified electrode was convenient for a simultaneous detection of Pb^{2+} and Cd^{2+} ions in aqueous solution, and it was successfully regenerated by immersion in NaCl solution (Fig. 14). The regenerated electrode was still effective for the ion detection (Fig. 14). However, the anodic current intensities related to Cd^{2+} and Pb^{2+} ions decreased of about 57 and 48%, respectively. The remaining electrochemical parameter change was less than 10%. It appeared that the decrease of the anodic current was essentially due to a partial alteration of the electrode by deactivation of a portion of the bentonite active sites.

Conclusion

The results obtained from this study allowed us to conclude that the bentonite-modified electrode sensitivity regarding Cd^{2+} ion detection was markedly affected by the change of the operating factors: solution pH, bentonite content, analyte concentration, electrolytes, and sweep rate. In alkaline media (up to pH = 9), a portion of cadmium-derivative cations seemed to be immobilized by the negatively charged clay particles, and consequently, the current signal diminished. In such a condition, the charge transfer was almost reversible. The current signal enhanced as the clay content increased, due to the good physical characteristics of the used clay minerals. However, because of the electrode peeling off, the bentonite content should not exceed 20 mass%. The relationship between the anodic current density and the cadmium cation initial concentration together with the cation exchange capacity of the electrode allowed us to conclude that the electrode's limit of detection fell within the range of 6×10^{-6}–5×10^{-5} M. The calculated values of LOD and LOQ (4.23×10^{-7}M and 1.41×10^{-6}M, respectively) supported the latter conclusion. The effect of the tested supporting electrolytes on the electrochemical performance of the electrode was essentially linked to the cation exchange process and the clay mineral protonation. In this connection, it should be noted that the use of HCl as a supporting electrolyte significantly improved the electrochemical performance of the studied electrode. The electron transfer process exhibited a transition from quasi-reversible to irreversible behavior when the sweep rate exceeded 50 mV/s. This change was accompanied by the disappearance of the cathodic peak and an intensification of the anodic current density.

The bentonite, as an electrode modifier, facilitated the electrode regeneration through leaching with a salt aqueous solution. The regeneration process seemed to occur by cation exchange. The regenerated electrode exhibited successful reusability. On the other hand, the studied electrode showed excellent sensitivity and high selectivity regarding the simultaneous detection of Cd^{2+} and Pb^{2+} ions.

The electrical equivalent circuit of the electrode-solution interface consisted of a double-layer capacitance in parallel with an electron transfer resistance and a Warburg impedance. This model accurately described the electrical behavior of the electrode during the electrochemical process.

These findings, which highlighted the suitability of the bentonite-carbon paste working electrode for cadmium detection, contribute to the advancement of electrochemical sensing techniques and can help to extend the clay-modified electrode use for heavy metal detection.

References

1. López JE, Arroyave C, Aristizábal A, Almeida B, Builes S, Chavez E (2022) Reducing cadmium bioaccumulation in Theobroma cacao using biochar: basis for scaling-up to field. Heliyon 8(6):e09790
2. Zhang Y, Wu Y, Song B, Zhou L, Wang F, Pang R (2022) Spatial distribution and main controlling factor of cadmium accumulation in agricultural soils in Guizhou. China J Hazard Mater 424:127308
3. Wang Y, Xing W, Liang X, Xu Y, Wang Y, Huang Q, Li L (2022) Effects of exogenous additives on wheat Cd accumulation, soil Cd availability and physicochemical properties in Cd-contaminated agricultural soils: a meta-analysis. Sci Total Environ 808:152090
4. Agyeman PC, Borůvka L, Kebonye NM, Khosravi V, John K, Drabek O, Tejnecky V (2023) Prediction of the concentration of cadmium in agricultural soil in the Czech Republic using legacy data, preferential sampling, Sentinel-2, Landsat-8, and ensemble models. J Environ Manage 330:117194
5. Souza-Arroyo V, Fabián JJ, Bucio-Ortiz L, Miranda-Labra RU, Gomez-Quiroz LE, Gutiérrez-Ruiz MC (2022) The mechanism of the cadmium-induced toxicity and cellular response in the liver. Toxicology 480:153339
6. Li Y, Rahman SU, Qiu Z, Shahzad SM, Nawaz MF, Huang J, Naveed S, Li L, Wang X, Cheng H (2023) Toxic effects of cadmium on the physiological and biochemical attributes of plants, and phytoremediation strategies: a review. Environ Pollut 325:121433
7. Naksen P, Boonruang S, Yuenyong N, Lee HL, Ramachandran P, Anutrasakda W, Amatatongchai M, Pencharee S, Jarujamrus P (2022) Sensitive detection of trace level Cd (II) triggered by chelation enhanced fluorescence (CHEF)"turn on": nitrogendoped graphene quantum dots (N-GQDs) as fluorometric paper-based sensor. Talanta 242:123305
8. Blaise N, Gomdje Valéry H, Maallah R, Oubaouz M, Tigana Djonse Justin B, Andrew Ofudje E, Chtaini A (2022) Simultaneous electrochemical detection of Pb and Cd by carbon paste electrodes modified by activated clay. J Anal Methods Chem 2022
9. Thatikayala D, Noori MT, Min B (2023) Zeolite-modified electrodes for electrochemical sensing of heavy metal ions–progress and future directions. Mater Today Chem 29:101412

10. Selmi A, Khiari R, Snoussi A, Bouzouita N (2021) Analysis of minerals and heavy metals using ICP-OES and FTIR techniques in two red seaweeds (Gymnogongrus griffithsiae and Asparagopsistaxiformis) from Tunisia. Biol Trace Elem Res 199:2342–2350
11. Lemos VA, de Carvalho AL (2010) Determination of cadmium and lead in human biological samples by spectrometric techniques: a review. Environ Monit Assess 171:255–265
12. He Q, Wang B, Liang J, Liu J, Liang B, Li G, Long Y, Zhang G, Liu H (2023) Research on the construction of portable electrochemical sensors for environmental compounds quality monitoring. Mater Today Adv 17:100340
13. Hanrahan G, Patil DG, Wang J (2004) Electrochemical sensors for environmental monitoring: design, development and applications. J Environ Monit 6(8):657–664
14. Afsharara H, Asadian E, Mostafiz B, Banan K, Bigdeli SA, Hatamabadi D, Keshavarz A, Hussain CM, Keçili R, Ghorbani-Bidkorpeh F (2023) Molecularly imprinted polymer-modified carbon paste electrodes (MIP-CPE): a review on sensitive electrochemical sensors for pharmaceutical determinations. TrAC Trends Anal Chem 160
15. Mostafiz B, Bigdeli SA, Banan K, Afsharara H, Hatamabadi D, Mousavi P, Hussain CM, Keçili R, Ghorbani-Bidkorbeh F (2021) Molecularly imprinted polymer-carbon paste electrode (MIP-CPE)-based sensors for the sensitive detection of organic and inorganic environmental pollutants: a review. Trends Environ Anal Chem 32:e00144
16. Jayaprakash GK, Swamy BK, Rajendrachari S, Sharma SC, Flores-Moreno R (2021) Dual descriptor analysis of cetylpyridinium modified carbon paste electrodes for ascorbic acid sensing applications. J Mol Liq 334:116348
17. Shetti NP, Nayak DS, Reddy KR, Aminabhvi TM (2019) Graphene–clay-based hybrid nanostructures for electrochemical sensors and biosensors. In Graphene-based electrochemical sensors for biomolecules 235–274
18. Baranwal J, Barse B, Gatto G, Broncova G, Kumar A (2022) Electrochemical sensors and their applications: a review. Chemosensors 10(9):363
19. GadelHak Y, Hafez SH, Mohamed HF, Abdel-Hady EE, Mahmoud R (2023) Nanomaterials-modified disposable electrodes and portable electrochemical systems for heavy metals detection in wastewater streams: a review. Microchem J 193:109043
20. Muslim WA, Al-Nasri SK, Albayati TM (2023) Evaluation of bentonite, attapulgite, and kaolinite as eco-friendly adsorbents in the treatment of real radioactive wastewater containing Cs-137. Prog Nucl Energy 162:104730
21. Yıldız C, Bayraktepe DE, Yazan Z, Önal M (2022) Bismuth nanoparticles decorated on Na-montmorillonite-multiwall carbon nanotube for simultaneous determination of heavy metal ions-electrochemical methods. J Electroanal Chem 910:116205
22. Souza LP, Lima AR, Martins TA, Vicentini FC, Marcolino-Junior LH, Bergamini MF (2023) Electrochemical determination of vitamin B12 (cyanocobalamin) using mercury nanodroplets supported at montmorillonite on a carbon paste electrode (CPE) Anal Lett 1–16
23. Caglar B, GunerEK KK, Özdokur KV, Cubuk O, Coldur F, CaglarS TopcuC, Tabak A (2018) Fe_3O_4 nanoparticles decorated smectite nanocomposite: characterization, photocatalytic and electrocatalytic activities. Solid State Sci 83:122–136
24. Tsotsou GE, Mazarakis AP (2023) Prospects and limitations of a clay-enabled pre-concentration method for spectrophotometric quantification. Appl Clay Sci 233:106829
25. Jaber L, Elgamouz A, Kawde AN (2022) An insight to the filtration mechanism of Pb (II) at the surface of a clay ceramic membrane through its preconcentration at the surface of a graphite/clay composite working electrode. Arab J Chem 15(12):104303
26. Jlassi K, Al Ejji M, Ahmed AK, Mutahir H, Sliem MH, Abdullah AM, Chehimi MM, Krupa I (2023) A carbon dot-based clay nanocomposite for efficient heavy metal removal. Nanoscale Adv 5:4224–4232
27. Beltagi AM, Ismail IM, Ghoneim MM (2013) Square-wave adsorptive cathodic stripping voltammeteric determination of manganese (II) using a carbon paste electrode modified with montmorillonite clay. Am J Anal Chem 4(4):30455
28. Guenang LS, Dongmo LM, Jiokeng SL, Kamdem AT, Doungmo G, Tonlé IK, Bassetto VC, Jović M, Lesch A, Girault H (2020) Montmorillonite clay-modified disposable ink-jet-printed graphene electrode as a sensitive voltammetric sensor for the determination of cadmium (II) and lead (II). SN Appl Sci 2:1–13
29. Aran D, Maul A, Masfaraud JF (2008) A spectrophotometric measurement of soil cation exchange capacity based on cobaltihexamine chloride absorbance. CR Geosci 340(12):865–871
30. Ilkhomidinovich MI (2019) Study of the sorption and textural properties of bentonite and kaolin. Austrian J Tech Nat Sci 11–12:33–37
31. Matusik J, Koteja-KuneckaA MP, Kunecka A (2022) Styrene removal by surfactant-modified smectite group minerals: efficiency and factors affecting adsorption/desorption. Chem Eng J 428:130848
32. Lu HL, Li KW, Nkoh JN, He X, Hong ZN, Xu RK (2022) Effects of the increases in soil pH and pH buffering capacity induced by crop residue biochars on available Cd contents in acidic paddy soils. Chemosphere 301:134674
33. Da Silva OB, Machado SA (2012) Evaluation of the detection and quantification limits in electroanalysis using two popular methods: application in the case study of paraquat determination. Anal Methods 4(8):2348–2354
34. Manisha H, Sonia J, Shashikiran S, Yuvarajan S, Rekha PD, Prasad KS (2022) Computer numerical control-printed paper electrodes for electrochemical detection of Pseudomonas aeruginosa virulence factor pyocyanin. Electrochem Commun 137:107259
35. Okpara EC, Fayemi OE, Sherif ESM, Ganesh PS, Swamy BK, Ebenso EE (2022) Electrochemical evaluation of Cd^{2+} and Hg^{2+} ions in water using ZnO/Cu_2ONPs/PANI modified SPCE electrode. Sens Bio-Sens Res 35:100476
36. Elgrishi N, Rountree KJ, McCarthy BD, Rountree ES, Eisenhart TT, Dempsey JL (2018) A practical beginner's guide to cyclic voltammetry. J Chem Educ 95(2):197–206
37. Coutinho I, Fortunato E (2018) A simple procedure to fabricate paper biosensor and its applicability—NADH/NAD^+ redox system. J Pharm Pharmacol 6:175–187
38. Xinxin MO, Siebecker MG, Wenxian GOU, Ling LI, Wei LI (2021) A review of cadmium sorption mechanisms on soil mineral surfaces revealed from synchrotron based X-ray absorption fine structure spectroscopy: implications for soil remediation. Pedosphere 31(1):11–27
39. Arun Kumar NS, Ashoka S, Malingappa P (2018) Nano zinc ferrite modified electrode as a novel electrochemical sensing platform in simultaneous measurement of trace level lead and cadmium. J Environ Chem Eng 6(6):6939–6946
40. Hwang JH, Wang X, Pathak P, Rex MM, Cho HJ, Lee WH (2019) Enhanced electrochemical detection of multiheavy metal ions using a biopolymer-coated planar carbon electrode. IEEE Trans Instrum Meas 68(7):2387–2393
41. Lalmalsawmi J, Tiwari D, Lee SM (2020) Low cost, highly sensitive and selective electrochemical detection of arsenic (III) using silane grafted based nanocomposites. Environ Eng Res 25(4):579–587
42. Aghris S, Matrouf M, Ettadili FE, Laghrib F, El Bouabi Y, Saqrane S, Farahi A, Bakasse M, Lahrich S, El Mhammedi MA (2021) Electrochemical analysis of flubendiamide in water and white rice using clay microparticles supported on pencil electrode. Microchem J 168:106486

43. Alves TS, Santos JS, Fiorucci AR, Arruda GJ (2019) A new simple electrochemical method for the determination of bisphenol a using bentonite as modifier. Mater Sci Eng, C 105:110048
44. Lalmalsawmi J, Tiwari D, Lee SM, Kim DJ (2021) Indigenously synthesized nanocomposite materials: use of nanocomposite as novel sensing platform for trace detection of Pb^{2+}. J Electroanal Chem 897:115578